Experimental Validation of a Closed Brayton Cycle System Transient Simulation

Presented at the Space Technology & Applications International Forum (STAIF-2006)
23rd Symposium on Space Nuclear Power and Propulsion
Albuquerque, New Mexico USA
February 15, 2006

Paul K. Johnson
Analex Corporation
Cleveland, OH 44135
Paul.K.Johnson@grc.nasa.gov

David S. Hervol
Analex Corporation
Cleveland, OH 44135
David.S.Hervol@grc.nasa.gov

Acknowledgement

The work in this paper was performed for NASA Headquarters, Prometheus Nuclear Systems Program. Any opinions expressed are those of the authors and do not necessarily reflect the views of the Prometheus Nuclear Systems Program. The authors would like to thank Michael Barrett, Arthur Birchenough, Michael Johnston, and Lee Mason for their assistance with testing and analysis.

Outline

- Introduction
- Brayton hardware
- Brayton testing
- Computer model description
- Steady-state model comparison
- Transient model description
- Conclusions

Introduction

- The Brayton Power Conversion Unit (BPCU) is a closed cycle system with an inert gas working fluid
  - Located in Vacuum Facility 6 at NASA Glenn Research Center
- Used in previous solar dynamic technology efforts (SDGTD)
  - Modified to its present configuration by replacing the solar receiver with an electrical resistance heater
- The first closed-Brayton-cycle to be coupled with an ion propulsion system (STAIF 2004)
- Used to examine mechanical dynamic characteristics and responses (STAIF 2005)
- The focus of this work was the validation of a computer model of the BPCU
  - Model was built using the Closed Cycle System Simulation (CCSS) design and analysis tool
  - Test conditions were then duplicated in CCSS
  - Various steady-state points
  - Transients involving changes in shaft rotational speed and heat input

Brayton Hardware

- Designed for operation up to 2 kWe output power
- Fully integrated power conversion system
  - Turbine-alternator-compressor (radial/centrifugal)
    - Gas cooled alternator and shaft
    - Gas foil bearings
  - Recuperator
    - Hastelloy X construction
    - Offset strip-fin, counter-flow
    - 97.5% effective
  - Gas cooler and commercial chiller (pumped ethylene glycol)
    - Stainless steel and nickel construction
    - Offset strip-fin, counter-flow
  - Electric resistance heater
    - Three silicon-carbide heating elements encapsulated in three finned metal tubes
    - Haynes 188 construction
    - Gas temperatures in excess of 1000 K
- Helium-Xenon working fluid
  - 62.7 mole % Helium, 37.3 mole % Xenon (83.8 g/mol)
- Operated in a rough vacuum test environment
  - Hot components are covered with multi-foil insulation (MFI)

BPCU Hardware

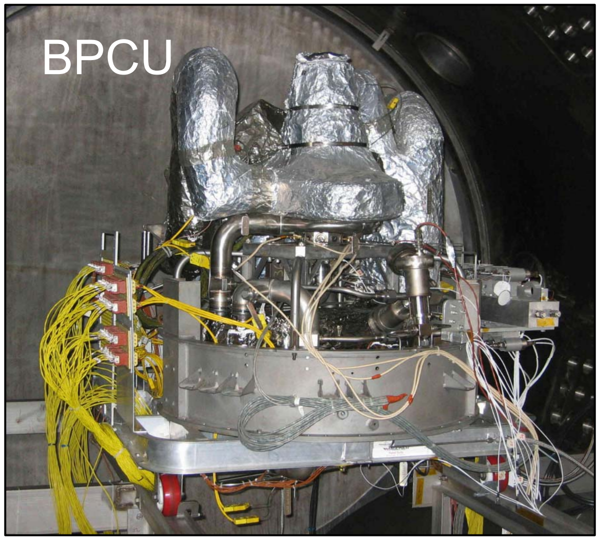

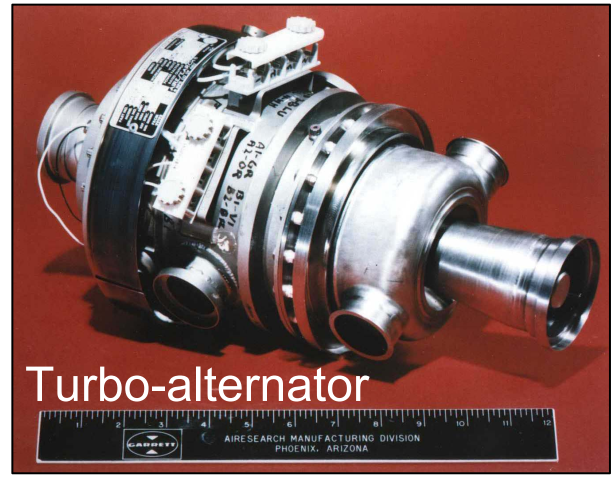

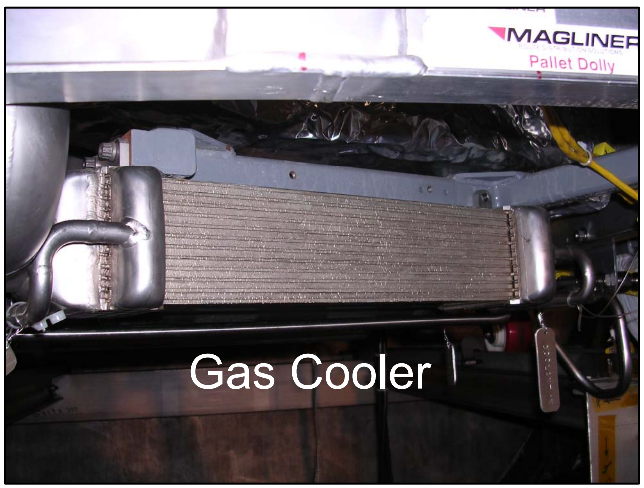

Brayton Test Matrix

- There are two primary variables used in operating the BPCU
  - Heater electrical power setting
  - Rotor speed setting
- Testing involved 12 transients
  - Changed step-wise heater power setting and rotor speed setting
  - System allowed to reach steady-state after each set-point step change

Positive Step Change Transients		Negative Step Change Transients	
Heater Power (kW)	Rotor Speed (kRPM)	Heater Power (kW)	Rotor Speed (kRPM)
4	28-37	8-6	52
4-5	37	6	52-46
5	37-46	6-5	46
5-6	46	5	46-37
6	46-52	5-4	37
6-8	52	4	37-28

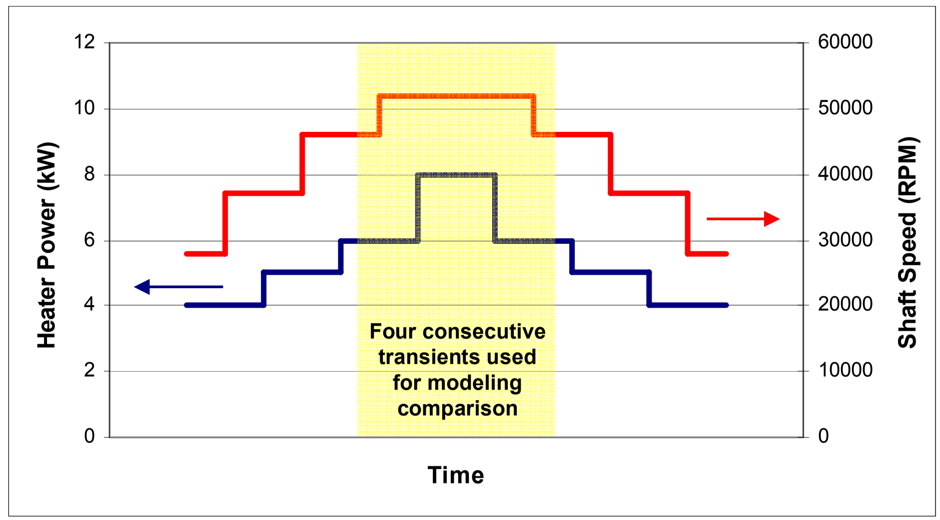

BPCU Test Results

- Steady-state results at three operating points for multiple runs
- Temperature variation was within +2.64 / - 2.55 %
- Pressure variation was within +2.14 / -2.67%
- BPCU demonstrated repeatability

	37 kRPM 4 kW		46 kRPM 5 kW		52 kRPM 8 kW	
Location	Average	(% +/-)	Average	(% +/-)	Average	(% +/-)
Heater Exit (K)	913	+1.20 / -1.65	862	+2.33 / -2.21	985	+0.63 / -0.63
Turbine Inlet (K)	915	1.24 / 1.82	865	2.55 / 2.43	988	0.64 / 0.64
Turbine Exit (K)	832	1.19 / 1.75	766	2.49 / 2.36	848	0.62 / 0.62
Recup. LP Inlet (K)	830	1.20 / 1.76	764	2.50 / 2.38	846	0.63 / 0.63
Recup. LP Exit (K)	356	0.41 / 0.86	371	0.88 / 0.85	396	0.21 / 0.21
Compressor Inlet (K)	285	0.06 / 0.09	284	0.12 / 0.07	285	0.03 / 0.03
Compressor Exit (K)	330	0.14 / 0.20	350	0.20 / 0.18	371	0.04 / 0.04
Recup. HP Inlet (K)	335	0.19 / 0.34	355	0.35 / 0.31	377	0.08 / 0.08
Recup. HP Exit (K)	815	1.23 / 1.88	751	2.63 / 2.53	830	0.66 / 0.66
Heater Inlet (K)	816	1.24 / 1.90	751	2.64 / 2.55	829	0.66 / 0.66
Compressor Inlet (kPa)	434	1.83 / 1.46	393	2.16 / 2.58	400	0.34 / 0.34
Compressor Exit (kPa)	552	2.05 / 1.46	572	2.14 / 2.55	634	0.25 / .025
Recup. HP Inlet (kPa)	552	1.92 / 1.47	565	2.06 / 2.61	634	0.31 / 0.31
Heater Inlet (kPa)	545	1.88 / 1.50	558	2.07 / 2.67	627	0.33 / 0.33
Heater Exit (kPa)	545	1.91/ 1.44	558	2.08 / 2.58	621	0.31 / 0.31
Turbine Inlet (kPa)	545	1.90 / 1.48	558	2.11 / 2.63	621	0.31 / 0.31
Turbine Exit (kPa)	434	1.81 / 1.45	393	2.14 / 2.56	400	0.34 / 0.34

Computer Model

- The Closed Cycle System Simulation (CCSS)
  - Closed-Brayton-cycle design and analysis tool
    - Numerical Propulsion System Simulation (NPSS) modeling environment
  - Originated from the Glenn Research Center in-house legacy program Closed Cycle Engine Program (CCEP)
  - CCSS models all of the major BPCU components
  - Accounts for shaft bearing and windage losses and bleed flow paths
  - A representation of the BPCU system was constructed in CCSS
    - Simulated steady state and thermal transients cases and compared to test data
- The CCSS BPCU model can be operated in three different modeling modes
  - Design
    - Components are sized and cycle state points are specified to meet a desired performance point
  - Off-design
    - Hardware geometries are held fixed from the design case
    - Shaft rotational speed, gas inventory, heater power, and coolant temperature can be varied
  - Transient
    - Very similar to off-design mode
    - Duct, recuperator, and heater material temperatures become time-dependent, allowing thermal transients to be evaluated

System Schematic

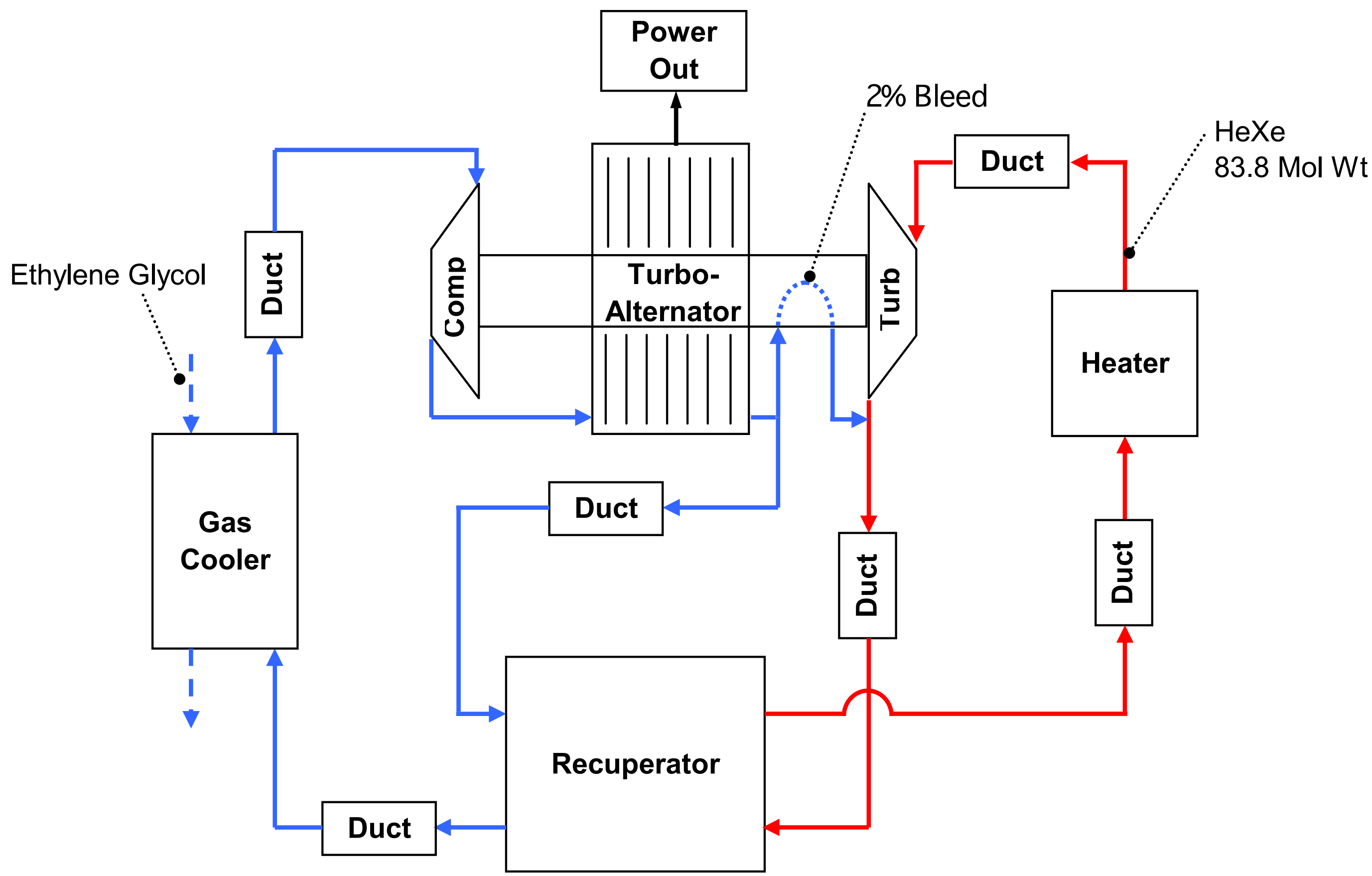

Model Components

- Ducts
  - Gas pressure drop and temperature change for each duct
  - Radiation heat loss is estimated
  - Duct material temperature is modeled with a lumped capacitance method

$$\frac{dT_{mat}}{dt} = \frac{Q_{in} - Q_{out}}{m_{mat} C_{mat}}$$

$$Q_{convec} = h_c A(T_{mat} - T_{gas})$$

$$Q_{rad} = \sigma A \varepsilon (T_{mat}^4 - T_{far}^4) \frac{1}{N_{layers} + 1}$$

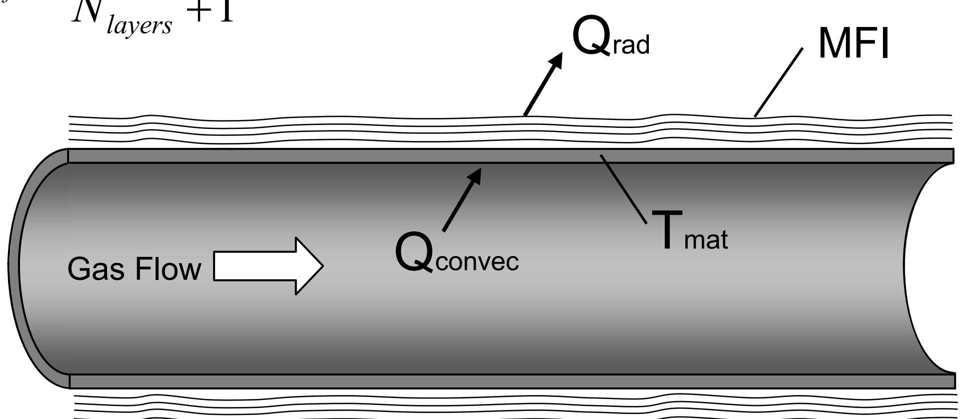

Model Components

- Recuperator
  - Gas pressure drop and temperature change
  - Radiation heat loss is estimated
  - Structure material temperature is modeled with a lumped capacitance method

$$\frac{dT_{mat}}{dt} = \frac{Q_{in} - Q_{out}}{m_{mat} C_{mat}}$$

$$Q_{convec} = h_c A (T_{mat} - T_{gas})$$

$$Q_{rad} = \sigma A \varepsilon (T_{mat}^4 - T_{far}^4) \frac{1}{N_{layers} + 1}$$

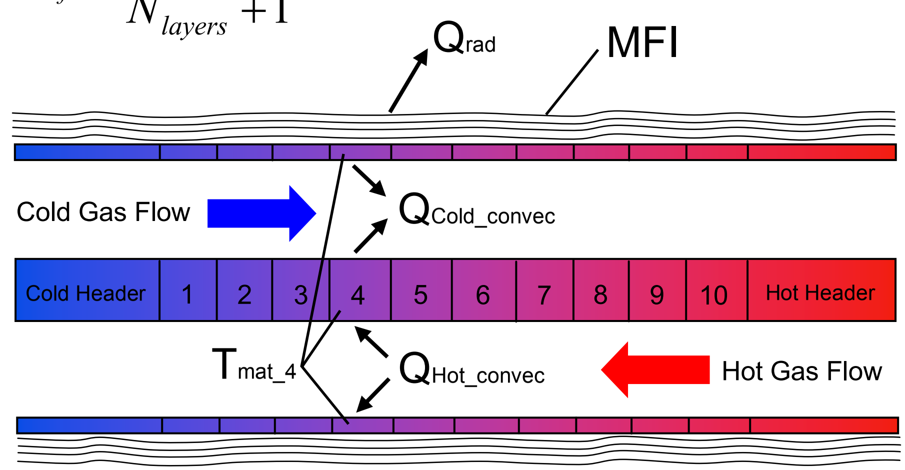

Model Components

- Heat source
  - Gas pressure drop and temperature change: $h_c A = fxn(\dot{m}, \mu)$ $\Delta P / P = fxn(\dot{m})$
  - Structure material temperature is modeled with a lumped capacitance method

$$\frac{dT_{mat}}{dt} = \frac{Q_{in} - Q_{out}}{m_{mat} C_{mat}}$$

$$Q_{convec} = h_c A(T_{mat} - T_{gas})$$

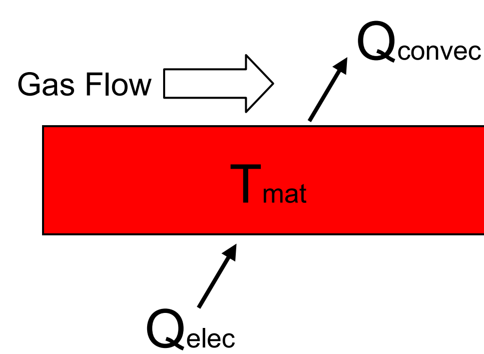

Model Components

- Gas cooler
  - Gas pressure drop and temperature change
  - Material temperature is not modeled in transient mode
- Turbine-alternator-compressor (TAC)
  - Performance maps estimate efficiency and pressure ratio for the turbine and compressor (from SDGTD literature)

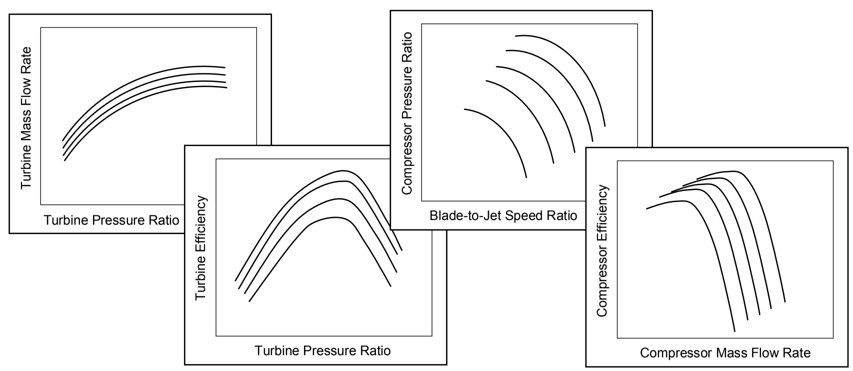

  - Alternator electromagnetic efficiency expressed as a function of shaft rotational speed and mechanical shaft power (from SDGTD literature)
  - Shaft windage (viscous drag) loss, thrust bearing loss, and journal bearing loss are estimated as functions of shaft cavity pressure and shaft rotational speed (from SDGTD literature)
  - TAC inertia not modeled for transient solutions

Matching Steady-State Data

- Gas inventory was set so that the heater exit pressure matched the test data
- Heater power was set so that the heater exit temperature matched the test data
  - Lower than the BPCU heater setting because heater losses not modeled
- Ethylene glycol temperature was set to match the BPCU compressor inlet temperature
- Shaft rotational speed was set to match the BPCU set point

	37 kRPM 4 kW			46 kRPM 5 kW			52 kRPM 8 kW		
Location	**Data**	**CCSS**	**%Diff**	**Data**	**CCSS**	**%Diff**	**Data**	**CCSS**	**%Diff**
Heater Exit (K)	913	913	0.00	868	868	0.00	978	978	0.00
Turbine Inlet (K)	915	908	-0.78	871	865	-0.78	982	974	-0.84
Turbine Exit (K)	832	834	0.23	772	770	-0.18	843	843	0.06
Compressor Inlet (K)	285	285	0.00	285	285	0.00	285	285	0.00
Compressor Exit (K)	330	325	-1.44	350	341	-2.73	371	355	-4.13
Recuperator HP Inlet (K)	335	333	-0.67	355	351	-1.11	377	368	-2.26
Heater Inlet (K)	817	816	-0.08	758	756	-0.33	823	826	0.32
Heater Cylinder (K)	936	937	0.09	903	906	0.27	1022	1016	-0.57
Heater Exit (kPa)	552	552	0.00	567	567	0.00	618	618	0.00
Turbine Inlet (kPa)	554	552	-0.39	569	567	-0.39	620	618	-0.42
Turbine Exit (kPa)	440	440	0.09	402	411	2.12	400	413	3.20
Turbine Pressure Ratio	1.26	1.25	-0.49	1.41	1.38	-2.45	1.55	1.5	-3.51
Compressor Inlet (kPa)	439	436	-0.63	400	406	1.30	397	407	2.36
Compressor Exit (kPa)	565	556	-1.46	581	573	-1.48	635	625	-1.56
Compressor Pressure Ratio	1.29	1.27	-0.83	1.45	1.41	-2.74	1.6	1.54	-3.83
Recuperator HP Inlet (kPa)	562	556	-0.94	578	572	-0.91	632	625	-1.05
Heater Inlet (kPa)	557	555	-0.39	573	571	-0.35	627	624	-0.53
Alternator Power (Watts)	413	382	-7.48	507	556	9.65	1141	1295	13.49

Matching Steady-State Data

- All of the CCSS temperatures were within 1% of the data
  - Exceptions were the compressor exit temperature and recuperator high pressure (HP) inlet temperature, which were lower than the data by as much as 4.1%
    - Likely the result of the CCSS compressor performance map underestimating pressure ratio and possibly overestimating efficiency
- Turbine and compressor pressure ratios were underestimated (between -0.39% and -3.83%), particularly at the higher shaft speeds
- Alternator power disagreed with the data by as much as 13.5%
  - Uncertainty in bearing and alternator loss estimates and compressor and turbine performance estimates
  - Compressor and turbine power are very sensitive to pressure ratio
    - Increase in compressor pressure ratio would result in more power consumed
    - Increase in turbine pressure ratio would result in more power produced by the turbine
    - Turbomachinery performance map errors and bearing and alternator loss uncertainties could easily account for the power differences indicated by the data

Matching Transient Data

- The BPCU system was operated at constant heater electric power and shaft rotational speed
- Transients were introduced to the system by changing stepwise the heater power and shaft speed set points
- Selected BPCU transient cases used for comparison
- CCSS model was anchored at the initial steady-state operating point
- CCSS was then switched to transient mode and shaft speed and heater power were changed stepwise as appropriate

BPCU Setpoints

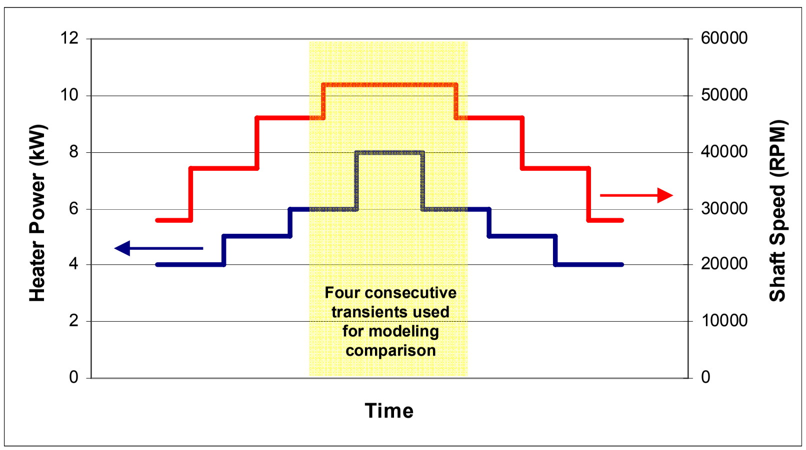

CCSS Setpoints

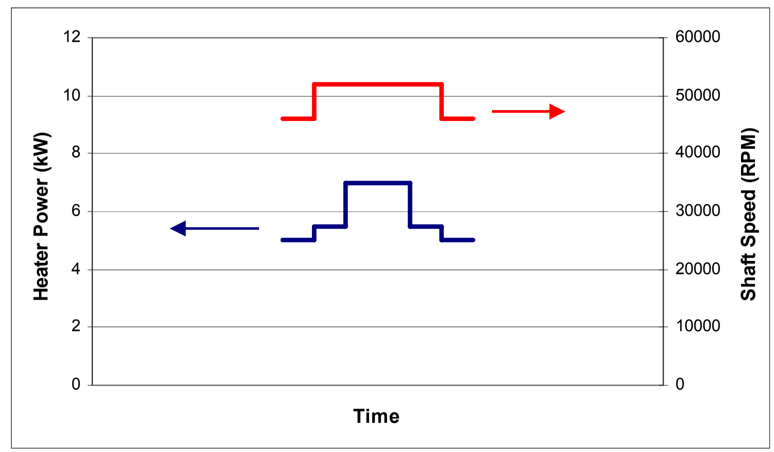

Matching Transient Data

- One would expect the CCSS heater exit temperature results to match the steady-state test data points (heater power was adjusted to do so)
- CCSS was ALSO able to match the shape of the transient curve between the steady-state points for both the heater inlet and heater exit temperatures
  - Captured the thermal response of system
- Shape of the recuperator material temperature plot also trends well with the data
  - Lumped capacitance method used to model the recuperator was appropriate
- Alternator power was overestimated by CCSS
  - The shape of the alternator power transient curve agrees well with the test data

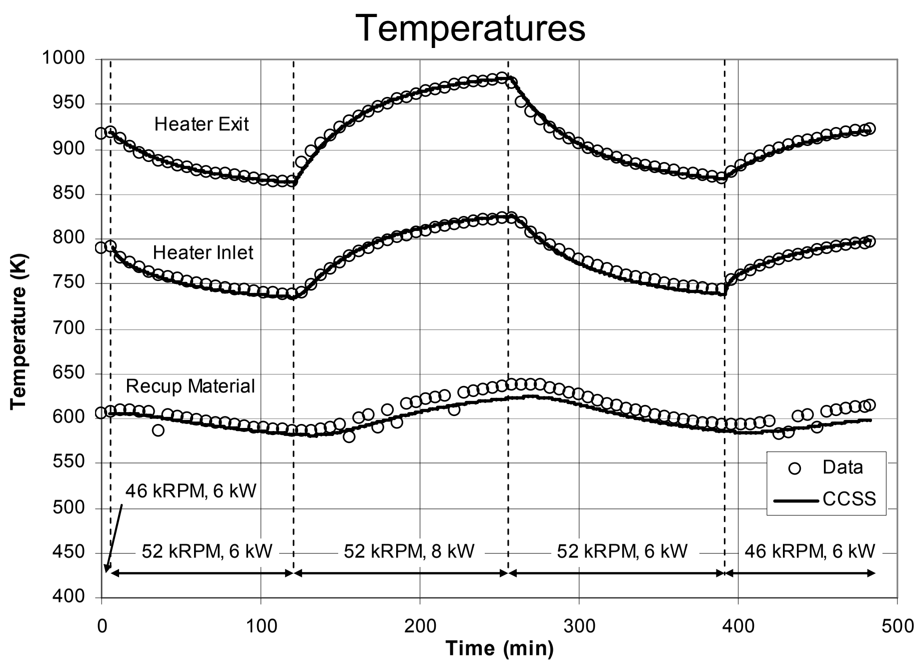

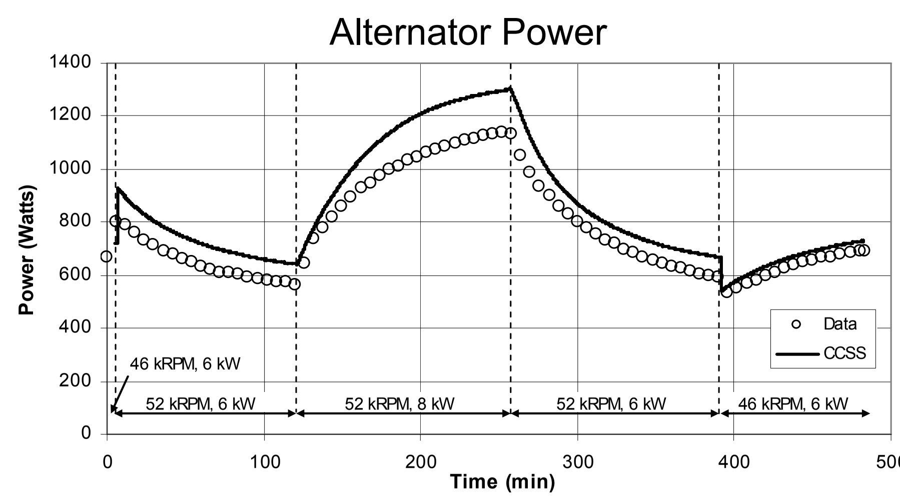

Component Transient Contributions

- Three thermal transient components
  - Gas ducts (11 kg total), Heater (38 kg), and Recuperator (59 kg)
- Determine component individual contributions to the system transient

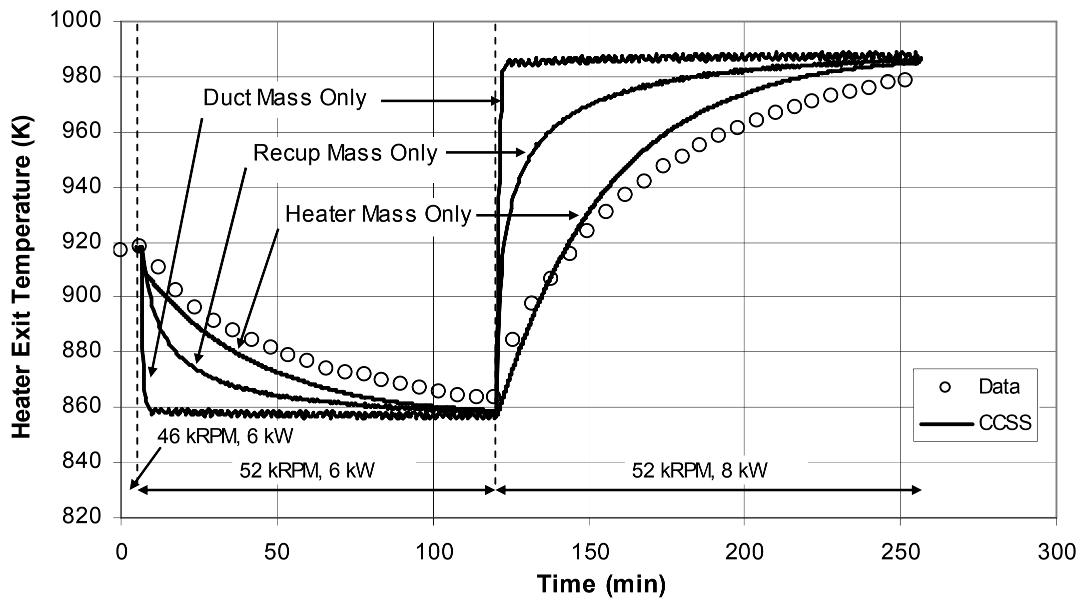

- Gas duct mass contributes very little to the overall system transient
- Heater contributes the most

Conclusions

- Testing to date has shown that the BPCU is able to generate meaningful, repeatable data that can be used for computer model validation
- Results generated by CCSS demonstrated that the model sufficiently reproduced the thermal transients exhibited by the BPCU system
- CCSS was also used to match BPCU steady-state operating points
  - Cycle temperatures were within 4.1% of the data (most were within 1%)
  - Cycle pressures were all within 3.2%
  - Error in alternator power (as much as 13.5%) was attributed to uncertainties in the compressor and turbine maps and alternator and bearing loss models
- The acquired understanding of the BPCU behavior gives useful insight for improvements to be made to the CCSS model as well as ideas for future testing and possible system modifications